SCALE-BASED FORMULATIONS OF STATISTICAL SELF-SIMILARITY IN IMAGES

Seungsin Lee

Center for Imaging Science
Rochester Institute of Technology
54 Lomb Memorial Drive
Rochester, NY 14623 USA

Raghuveer Rao

Department of Electrical Engineering
Rochester Institute of Technology
79 Lomb Memorial Drive
Rochester, NY 14623 USA

ABSTRACT

Statistically self-similar images that are segments of two dimensional self-similar random fields, have been useful in the analysis and synthesis of certain types of textures. Whereas a rigorous definition of self-similarity in continuous-space is based on spatial scaling, current treatments in digital image processing are based on ad-hoc approaches rather than on spatial scaling mainly because of the unavailability of continuous scaling in discrete-space. This paper presents a formulation based on such a continuous scaling operator leading to a more general and versatile characterization of statistical self-similarity in images.

1. INTRODUCTION

A two dimensional random field is statistically self-similar in the wide sense if its mean and autocorrelation functions are invariant to spatial scaling. Statistically self-similar images, which are segments of statistically self-similar random fields, have been useful in analyzing and synthesizing certain types of textures and natural patterns in various image processing areas [1–4].

Statistical self-similarity for continuous-space random fields has typically been defined in terms of isotropic scaling [5], or scaling by the same factors along both axes. Though this definition, which is a direct extension of the 1-D definition [5], is widely accepted for continuous-space self-similarity [6, 7], as we show in this paper, it is restrictive in the sense that various random fields that demonstrate aspects of self-similarity are not covered by it.

In discrete-space, a counterpart to the continuous-space definition does not exist because of the unavailability of continuous scaling in discrete-space. Therefore, other approaches have been utilized for discrete-space self-similar random fields instead of spatial scaling. A popular approach is to exploit characteristics of fractional Brownian (fBm) motion [8, 9]. A unique approach to defining self-similarity using a discrete-domain scaling operator was proposed by Zhao and Rao [10]. They devised a 1-D continuous scaling operation for discrete-time processes and applied it for 2-D self-similarity definition in discrete-space. However, that approach is also restrictive.

The key contributions of the paper are (1) it provides a definition for statistical self-similarity in continuous-space that is more general than the current definition, (2) it develops a formalism for self-similarity based on scaling that works in discrete-space rather than continuous-space, and (3) it provides examples of images synthesized using the new model.

This work was supported in part by grant HE–1442–2003 from the Xerox UAC foundation.

The paper is organized as follows. Section 2 proposes a new definition of the generalized self-similarity in continuous space. Section 3 provides a formulation which conducts the scaling operation in discrete-space, and offers a new definition for wide-sense discrete self-similar random fields. The algorithm to generate the discrete-space self-similar random fields and synthesis examples are provided in Section 4. Concluding remarks are drawn in Section 5.

2. GENERALIZED SELF-SIMILARITY IN CONTINUOUS SPACE

A generally accepted definition of the statistical self-similarity of a continuous-space random field $x(\mathbf{t})$, $\mathbf{t} = [t_1, t_2]^T$ is [5]

$$x(a\mathbf{t}) \stackrel{d}{=} a^H x(\mathbf{t}), \quad a > 0, \tag{1}$$

where, $\stackrel{d}{=}$ denotes equality of the finite-dimensional distributions and H is called the Hurst parameter.

However, the definition in (1) is restrictive in capturing certain types of self-similarity because it is simply a direct adoption of the 1-dimensional definition of self-similarity, and does not use the additional degree of freedom obtained by moving into 2 dimensions. Such limitations can be surmounted by defining self-similarity in a new way using a scaling operation by a matrix instead of a scalar factor as in (1)

Definition 1. *A random field $x(\mathbf{t})$ is self-similar for a matrix class $\mathcal{C}$ with index H if, for a non-singular matrix $\mathbf{A} \in \mathcal{C}$,*

$$x(\mathbf{At}) \stackrel{d}{=} |D|^{H/2} x(\mathbf{t}) \tag{2}$$

where $D = \det \mathbf{A}$.

We have chosen to use the term *index* instead of Hurst parameter to prevent confusion with earlier definitions. The definition in (1) is a special case of the new definition in (2) and holds for the class of diagonal matrices with equal entries, i. e., matrices of the form, $\mathbf{A} = a\mathbf{I}$, $a > 0$, where $\mathbf{I}$ is a 2 by 2 identity matrix. However, the new definition is more general than the definition in (1). For example, suppose a random field $h(t_1, t_2) = f(t_1)g(t_2)$ is composed of two independent random processes $f(t)$ and $g(t)$, where only $f(t)$ is self-similar with H. Obviously, $h(t_1, t_2)$ is directionally self-similar but this directional self-similarity cannot be captured by (1). On the contrary, according to the new definition, $h(\mathbf{t})$ is self-similar with respect to the class of matrices

$$\mathbf{A} = \begin{bmatrix} a & 0 \\ 0 & 1 \end{bmatrix}, \quad a > 0. \tag{3}$$

3. SCALING OPERATION AND STATISTICAL SELF-SIMILARITY IN DISCRETE-SPACE

We now formulate a scaling operator in discrete-space that leads to developing a framework for treating self-similarity on lines analogous to that for continuous space as in (2). Let $f(\omega)$ be a 1-D warping function that transforms a frequency $\omega \in [-\pi, \pi]$ to $\Omega \in [-\infty, \infty]$, where ω may be regarded as the frequency variable in the discrete time Fourier transform of a discrete time signal while Ω is the same for the continuous time Fourier transform of a continuous time signal [11]. Then the vector valued function

$$\boldsymbol{\Omega} = \mathbf{f}(\boldsymbol{\omega}) \triangleq [\Omega_1, \Omega_2]^T = [f(\omega_1), f(\omega_2)]^T \tag{4}$$

is a *2-D frequency warping transform*. Inversely, the unwarping transform $\mathbf{f}^{-1}(\boldsymbol{\Omega})$ maps $\boldsymbol{\Omega}$ into $\boldsymbol{\omega}$.

Based on the warping transform defined above, we define a scaling operation $\mathcal{T}_{\mathbf{A}}[\,]$ in 2-D discrete-space. Let $\mathbf{n} = [n_1, n_2]^T$. The scaling operation $\mathcal{T}_{\mathbf{A}}[\,]$ by a non-singular matrix $\mathbf{A}$ in 2-D discrete-space associated with a 2-D warping transform $\mathbf{f}$ is defined by the following input-output relationship:

$$y(\mathbf{n}) = \mathcal{T}_{\mathbf{A}}[x(\mathbf{n})] \triangleq \mathcal{G}^{-1}\left[|D| X(\boldsymbol{\Lambda}_{\mathbf{A}}(\boldsymbol{\omega}))\right], \tag{5}$$

where $D = \det \mathbf{A}$,

$$\boldsymbol{\Lambda}_{\mathbf{A}}(\boldsymbol{\omega}) \triangleq [\Lambda_1(\omega_1, \omega_2), \Lambda_2(\omega_1, \omega_2)]^T = \mathbf{f}^{-1}[\mathbf{A}^T \mathbf{f}(\omega)], \tag{6}$$

and $X(\boldsymbol{\omega})$ is a Fourier transform representation of $x(\mathbf{n})$ defined as

$$X(\boldsymbol{\omega}) = \mathcal{G}[x(\mathbf{n})] \triangleq \sum_{\mathbf{n}} x(\mathbf{n}) e^{-j\mathbf{n}\cdot\boldsymbol{\omega}} \tag{7}$$

with

$$x(\mathbf{n}) = \mathcal{G}^{-1}[X(\boldsymbol{\omega})] \triangleq \frac{1}{(2\pi)^2} \int_{\boldsymbol{\omega}} X(\boldsymbol{\omega}) e^{j\mathbf{n}\cdot\boldsymbol{\omega}}\, d\boldsymbol{\omega}. \tag{8}$$

We now define discrete-space statistical self-similarity in the wide-sense using the scaling operation $\mathcal{T}_{\mathbf{A}}$.

Definition 2. *A discrete-space random field $x(\mathbf{n})$ is self-similar for a matrix class C with the index H in the wide-sense if, for a non-singular matrix $\mathbf{A} \in C$,*

$$\begin{aligned} E[\mathcal{T}_{\mathbf{A}}[x(\mathbf{n})]] &= |D|^{-H/2} E[x(\mathbf{n})] \\ \mathcal{T}_{\mathbf{AA}}[R_{xx}(\mathbf{n}, \mathbf{n}')] &= |D|^{-H} R_{xx}(\mathbf{n}, \mathbf{n}') \end{aligned} \tag{9}$$

where $E[\,]$ is the mean of a random field and $R_{xx}(\mathbf{n}, \mathbf{n}')$ is the autocorrelation of the random field $x(\mathbf{n})$.

If the random field is zero-mean wide-sense stationary, the definition in (9) can be reduced to

$$\frac{P_x[\boldsymbol{\Lambda}_{\mathbf{A}}(\boldsymbol{\omega})]}{\left|\det\left[\frac{d\boldsymbol{\Lambda}_{\mathbf{A}}(\boldsymbol{\omega})}{d\boldsymbol{\omega}}\right]\right|} = |D|^{-H-2} P_x(\boldsymbol{\omega}). \tag{10}$$

where

$$\frac{d\boldsymbol{\Lambda}_{\mathbf{A}}(\boldsymbol{\omega})}{d\boldsymbol{\omega}} \triangleq \begin{bmatrix} \frac{\partial \Lambda_1(\omega_1,\omega_2)}{\partial \omega_1} & \frac{\partial \Lambda_2(\omega_1,\omega_2)}{\partial \omega_1} \\ \frac{\partial \Lambda_1(\omega_1,\omega_2)}{\partial \omega_2} & \frac{\partial \Lambda_2(\omega_1,\omega_2)}{\partial \omega_2} \end{bmatrix}. \tag{11}$$

For the rest of this paper, we only consider zero-mean wide-sense stationary random fields.

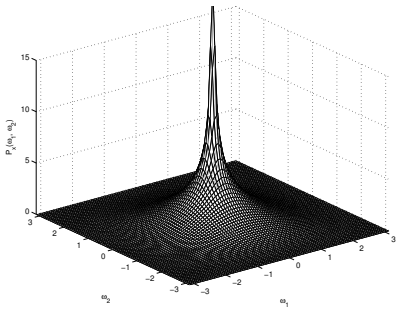

Fig. 1. Power spectrum P_1 with $r = -0.6$

One example of such a self-similar random field is a stationary random field $x_1(\mathbf{n})$ with the power spectrum

$$P_1(\boldsymbol{\omega}) = \frac{\|\mathbf{f}(\boldsymbol{\omega})\|^r}{\left|\det\left[\frac{d\,\mathbf{f}(\boldsymbol{\omega})}{d\,\boldsymbol{\omega}}\right]\right|}, \tag{12}$$

where, $\|\cdot\|$ denotes Euclidian norm. It can be shown that the random field $x_1(\mathbf{n})$ is self-similar with respect to

$$\mathbf{A}_1 = a \begin{bmatrix} \cos\theta & -\sin\theta \\ \sin\theta & \cos\theta \end{bmatrix} \tag{13}$$

with $H = -\frac{r}{2} - 1$.

Fig. 1 shows the power spectrum with $r = -0.6$ ($H = -0.7$) and the bilinear warping transform (BLT)

$$\mathbf{f}(\boldsymbol{\omega}) = [2\tan(\omega_1/2), 2\tan(\omega_2/2)]^T. \tag{14}$$

Notice that the range of the index H differs from the range of the Hurst parameter in continuous-space ($0 < H < 1$). Unlike the continuous case, discrete-random fields with the power spectrum in (12) are stationary.

Another example is the directionally self-similar random field $x_2(\mathbf{n})$ with the power spectrum

$$P_2(\omega_1, \omega_2) = \frac{|f(\omega_1)|^r}{|f'(\omega_1)|} g(\omega_2) \tag{15}$$

where $g(\omega)$ is an arbitrary 1-D power spectrum. Then $x_2(\mathbf{n})$ is self-similar with the index $H = -r - 1$ with respect to the class of matrices

$$\mathbf{A}_2 = \begin{bmatrix} a & 0 \\ 0 & 1 \end{bmatrix}, \quad a > 0. \tag{16}$$

The power spectrum $P_2(\boldsymbol{\omega})$ with $f(\omega) = 2\tan(\omega/2)$, $g(\omega) = 0.5(1 + \cos\omega)$ and $r = -1.2$ is shown in Fig. 2 (a). Note that $P_2(\boldsymbol{\omega})$ is infinity at $(0, \omega_2)$ when $r < 0$. The plot in Fig. 2 (a) excludes this frequency for the purpose of display.

To introduce our third example, we need the following theorem.

Theorem 1. *Let $P_x(\boldsymbol{\omega})$ be a power spectrum of a discrete-space random field $x(\mathbf{n})$ that is self-similar with index H with respect to a matrix class $\mathbf{A}$ according to* (10)*. Then, a stationary random field $y(\mathbf{n})$ with a power spectrum*

$$P_y(\boldsymbol{\omega}) = \left|\det \frac{d\boldsymbol{\omega}}{d\boldsymbol{\Lambda}_{\mathbf{C}}(\boldsymbol{\omega})}\right| P_x[\boldsymbol{\Lambda}_{\mathbf{C}}(\boldsymbol{\omega})] \tag{17}$$

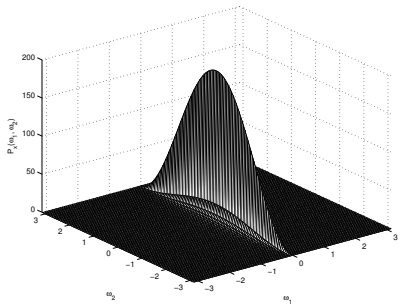

Fig. 2. Power spectrum of the directionally self-similar random field ($r = -1.2$)

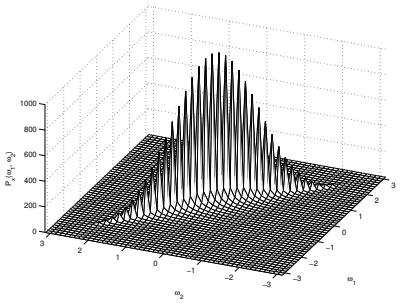

Fig. 3. Power spectrum P_2 of the oriented directionally self-similar random field ($r = -1.2$, $\theta_c = \pi/4$)

is self-similar with index H with respect to the class of matrices

$$\mathbf{B} = \mathbf{C}\mathbf{A}\mathbf{C}^T, \tag{18}$$

where $\mathbf{C}$ is an orthogonal matrix satisfying $\mathbf{C}\mathbf{C}^T = \mathbf{I}$.

Proof. Since $\mathbf{\Lambda_A}[\mathbf{\Lambda_B}(\boldsymbol{\omega})] = \mathbf{f}^{-1}[(\mathbf{BA})^T\mathbf{f}(\boldsymbol{\omega})] = \mathbf{\Lambda_{BA}}(\boldsymbol{\omega})$, for a self-similar random field $x(\mathbf{n})$,

$$\begin{aligned}
P_y(\mathbf{\Lambda_B}(\boldsymbol{\omega})) &= \left|\det \frac{d\mathbf{\Lambda_B}(\boldsymbol{\omega})}{d\mathbf{\Lambda_C}[\mathbf{\Lambda_{CAC}}^T(\boldsymbol{\omega})]}\right| P_x[\mathbf{\Lambda_C}(\mathbf{\Lambda_{CAC}}^T(\boldsymbol{\omega}))] \\
&= \left|\det \frac{d\mathbf{\Lambda_B}(\boldsymbol{\omega})}{d\mathbf{\Lambda_{CA}}(\boldsymbol{\omega})}\right| P_x[\mathbf{\Lambda_{CA}}(\boldsymbol{\omega})] \\
&= \left|\det \frac{d\mathbf{\Lambda_B}(\boldsymbol{\omega})}{d\mathbf{\Lambda_A}(\mathbf{\Lambda_C}(\boldsymbol{\omega}))}\right| \left|\det \frac{d\mathbf{\Lambda_A}(\mathbf{\Lambda_C}(\boldsymbol{\omega}))}{d\mathbf{\Lambda_C}(\boldsymbol{\omega})}\right| \\
&\times |D_{\mathbf{A}}|^{-H-2} P_x[\mathbf{\Lambda_C}(\boldsymbol{\omega})] \\
&= \left|\det \frac{d\mathbf{\Lambda_B}(\boldsymbol{\omega})}{d\mathbf{\Lambda_C}(\boldsymbol{\omega})}\right| |D_{\mathbf{A}}|^{-H-2} \frac{P_y(\boldsymbol{\omega})}{\left|\det \frac{d\boldsymbol{\omega}}{d\mathbf{\Lambda_C}(\boldsymbol{\omega})}\right|} \\
&= \left|\det \left[\frac{d\mathbf{\Lambda_B}(\boldsymbol{\omega})}{d\boldsymbol{\omega}} \frac{d\boldsymbol{\omega}}{d\mathbf{\Lambda_C}(\boldsymbol{\omega})} \left(\frac{d\boldsymbol{\omega}}{d\mathbf{\Lambda_C}(\boldsymbol{\omega})}\right)^{-1}\right]\right| \\
&\times |D_{\mathbf{A}}|^{-H-2} P_y(\boldsymbol{\omega}) \\
&= \left|\det \frac{d\mathbf{\Lambda_B}(\boldsymbol{\omega})}{d\boldsymbol{\omega}}\right| |D_{\mathbf{A}}|^{-H-2} P_y(\boldsymbol{\omega}).
\end{aligned}$$

Furthermore, since $\mathbf{C}$ is an orthogonal matrix, $|D_{\mathbf{B}}| = |D_{\mathbf{A}}|$, and

$$\frac{P_y(\mathbf{\Lambda_B}(\boldsymbol{\omega}))}{\left|\det \frac{d\mathbf{\Lambda_B}(\boldsymbol{\omega})}{d\boldsymbol{\omega}}\right|} = |D_{\mathbf{B}}|^{-H-2} P_y(\boldsymbol{\omega}). \tag{19}$$

□

With $P_x(\boldsymbol{\omega}) = P_2(\boldsymbol{\omega})$ and

$$\mathbf{C} = \begin{bmatrix} \cos\theta_c & -\sin\theta_c \\ \sin\theta_c & \cos\theta_c \end{bmatrix}, \tag{20}$$

$P_y(\boldsymbol{\omega})$ becomes the power spectrum for directional random fields rotated by an angle θ_c. The power spectrum $P_y(\boldsymbol{\omega})$ is depicted in Fig. 3. The plot was generated with the same $f(\omega)$ and $g(\omega)$ as in $P_2(\boldsymbol{\omega})$ with $\theta_c = \pi/4$. Again, infinity values in the power spectrum were removed from the plot, which were located on the line $\omega_1 = -\omega_2$.

4. SYNTHESIS OF DISCRETE-SPACE SELF-SIMILAR RANDOM FIELDS

Construction of 1-D systems to generate 1-D discrete-time self-similar processes was possible by factorization of the corresponding power spectrum [11]. Unlike 1-D factorization, however, it is known that a rational 2-D spectrum cannot generally be factorized into rational factors. Ekstrom and Woods [12] provided an approach to achieve the factorization of a 2-D power spectrum through complex cepstrum, and it was used here to design a 2-D recursive filter for discrete-space self-similar random fields.

However, the cepstrum method cannot directly be applied to power spectra introduced here because they do not satisfy the condition for existence of the cepstrum stated in [12] in certain situations, especially when $r < 0$. Furthermore, the power spectra may have zero values at certain frequencies, which hinder to apply the logarithm to the power spectra. Therefore, we modify the power spectra with small constants. For instance, $P_1(\omega)$ in (12) can be approximated with $c_1, c_2 \ll 1$ as

$$\tilde{P}_1(\boldsymbol{\omega}) = \frac{\|\mathbf{f}(\boldsymbol{\omega}) + c_1\|^r}{\left|\det\left[\frac{d\,\mathbf{f}(\boldsymbol{\omega})}{d\,\boldsymbol{\omega}}\right]\right|} + c_2. \tag{21}$$

Then, the cepstrum based factorization can be applied to $\tilde{P}_1(\boldsymbol{\omega})$ to construct a recursive filter. Other power spectra can also be approximated in the similar way.

We first synthesize discrete self-similar random fields using the power spectrum $P_1(\boldsymbol{\omega})$ in (12) with the BLT in (14). As discussed, $P_1(\boldsymbol{\omega})$ is approximated as

$$\tilde{P}(\omega) = \frac{2^r[\tan^2(\frac{\omega_1}{2}) + \tan^2(\frac{\omega_2}{2}) + c_1]^{r/2}}{\sec^2(\frac{\omega_1}{2})\sec^2(\frac{\omega_2}{2})} + c_2. \tag{22}$$

Discrete-space self-similar random fields generated from white noise inputs with $r = -0.6$ ($H = -0.7$) and -1.4 ($H = -0.3$) are given Fig. 4.

Fig. 5 shows an example of a directionally self-similar random field from $P_2(\boldsymbol{\omega})$ in (15) with $f(\omega) = 2\tan(\omega/2)$, $g(\omega) = 0.5(1 + \cos(\omega))$, and $r = -1.2$. The directionality in the random fields can easily be observed from the synthesized images. Finally, Fig. 6 displays a directionally self-similar random field rotated with an angle $\theta_c = \pi/4$ and $r = -1.2$.

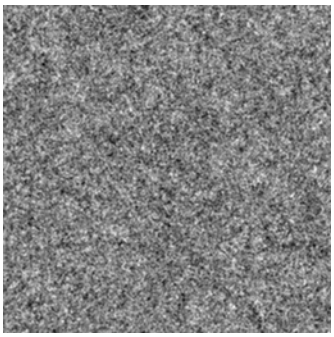

(a)

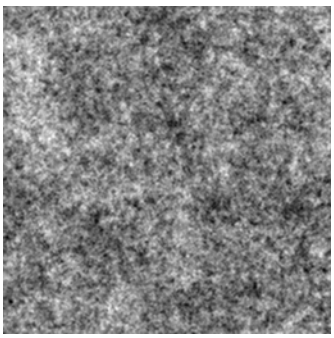

(b)

Fig. 4. Synthesized discrete self-similar images, (a) $r = -0.6$, (b) $r = -1.4$

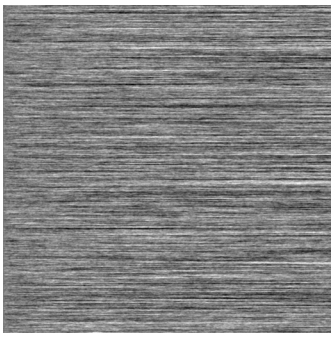

Fig. 5. Synthesized directionally self-similar images ($r = -1.2$)

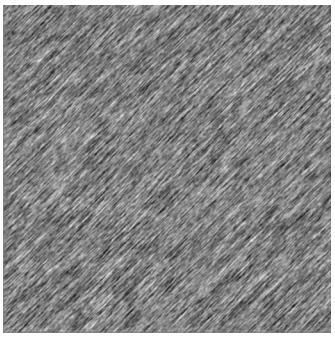

Fig. 6. Synthesized oriented directionally self-similar images with $\theta_c = \pi/4$, and $r = -1.2$

5. CONCLUSION

In this paper, we pointed out the limitation of the current statistical self-similarity definition in continuous-space and suggested a new definition. Self-similarity in discrete-space was formulated by a new scaling operation based on 2-D frequency warping transform. As a result, it is possible to describe the self-similarity of random fields, which would be considered not self-similar by previous definitions. Also, a wider class of self-similar fields can be synthesized based on the new self-similarity definition. Synthesis examples demonstrated that the new definition can generate various types of self-similar random fields such as directionally self-similar random fields in discrete-space.

6. REFERENCES

[1] C. V. Stewart, B. Moghaddam, K. J. Hintz, and L. M. Novak, "Fractional Brownian motion models for synthetic aperture radar imagery scene segmentation," *Proceedings of the IEEE*, vol. 81, no. 10, pp. 1511–1522, 1993.

[2] R. Jennane, W. J. Ohley, S. Majumdar, and G. Lemineur, "Fractal analysis of bone X-ray tomographic microscopy projections," *IEEE Trans. Med. Imag.*, vol. 20, no. 5, pp. 443–449, 2001.

[3] A. P. Pentland, "Fractal-based description of natural scenes," *IEEE Trans. Pattern Anal. Machine Intell.*, vol. PAMI-6, no. 6, pp. 661–674, 1984.

[4] L. M. Kaplan, "Extended fractal analysis for texture classification and segmentation," *IEEE Trans. Image Processing*, vol. 8, no. 11, pp. 1572–1585, 1999.

[5] G. Samorodnitsky and M. S. Taqqu, *Stable Non-Gaussian Random Processes : Stochastic Models with Infinite Variance*. New York: Chapman & Hall, 1994.

[6] K. J. Falconer and J. L. Véhel, "Horizons of fractional Brownian surfaces," *Proc. R. Soc. Lond. A*, vol. 456, pp. 2153–2178, 2000.

[7] B. Pesquet-Popescu and J. L. Véhel, "Stochastic fractal models for image processing," *Signal Processing*, vol. 19, no. 5, pp. 48–62, Sep. 2002.

[8] L. M. Kaplan and C. C. J. Kuo, "An improved method for 2-d self-similar image synthesis," *IEEE Trans. Image Processing*, vol. 5, no. 5, pp. 754–761, 1996.

[9] I. S. Reed, P. C. Lee, and T. K. Truong, "Spectral representation of fractional Brownian motion in *N* dimensions and its properties," *IEEE Trans. Inform. Theory*, vol. 41, no. 5, pp. 1439–1451, 1995.

[10] W. Zhao, "Discrete-time continuous-dilation construction of linear scale-invariant systems and multi-dimensional self-similar signals," Ph.D. dissertation, Rochester Institute of Technology, 1999.

[11] S. Lee, W. Zhao, R. Narasimha, and R. M. Rao, "Discrete-time models for statistically self-similar signals," *IEEE Trans. Signal Processing*, vol. 51, no. 5, pp. 1221–1230, 2003.

[12] M. Ekstrom and J. Woods, "Two-dimensional spectral factorization with applications in recursive digital filtering," *Acoustics, Speech, and Signal Processing*, vol. 24, no. 2, pp. 115–128, 1976.